PCCP

PAPER

View Article Online
View Journal | View Issue

Cite this: *Phys. Chem. Chem. Phys.*, 2019, **21**, 1190

The optical absorption spectra of spontaneously electrical solids: the case of nitrous oxide

Andrew Cassidy, *[a] Rachel L. James, [b] Anita Dawes, [b] Jérôme Lasne [c] and David Field [ad]

Received 11th September 2018,
Accepted 10th December 2018

DOI: 10.1039/c8cp05746j

rsc.li/pccp

Absorption spectra of films of N_2O, in the range 115–160 nm, are presented for deposition temperatures between 33 K and 64 K. Observed shifts in the absorption energy *vs.* deposition temperature are analysed in terms of the temperature-dependent spontaneously electrical ('spontelectric') fields present in the films. Using a simple electrostatic theory, we suggest that (i) spectra are associated with Wannier–Mott excitons, (ii) the action of the electric field upon the excitons suffers a blockade at $\leq$54 K for the C-state and $\leq$52 K for the D-state of N_2O, (iii) the blockade may be attributed to structural defects, which trap excitons, limiting their size and (iv) films form with defect-free regions containing 324 ± 3, 168 ± 46 and 95 ± 1 molecules of N_2O at 54 K, 52 K and 50 K respectively, yielding an experimental indication of the scale size of regular periodicity associated with Wannier–Mott excitons. Results demonstrate how the spontelectric effect can be used as a tool for exploring the structure of solids and give a graphic image of the structural changes that take place close to the known phase change at 47 K/48 K.

1. Introduction

The object of the current work is to shed light on the remarkable sensitivity of the electronic absorption spectra of ices of polar molecules to their deposition temperature, T_d.[1,2] For example, spectral features have previously been observed to change by hundreds of wavenumbers for a change in T_d of a few K in solid CO.[3] This phenomenon has recently been shown to be a consequence of the electrical characteristics of CO ices. Briefly, a variety of techniques, including direct measurement of surface potentials, and Stark effects in reflection–absorption infrared spectroscopy and vacuum-ultraviolet spectroscopy,[1,4–8] demonstrate the presence of substantial fields in vacuum deposited films of numerous polar species. Of particular relevance here, N_2O ices have been found spontaneously to display large internal electrical fields. The magnitude of these so-called 'spontelectric fields' depends on deposition temperature. Spontelectric fields in N_2O films vary, for example, between 6.32×10^7 V m^{-1} for films laid down at T_d = 50 K and 3.45×10^7 V m^{-1} for T_d = 62 K. We describe below how the shifts with T_d of peaks, in electronic absorption spectra of films of N_2O, are governed by variation of the spontelectric field, through corresponding Stark shifts of the excitons formed in VUV excitation. Quantitative connection is made between the known electric fields in the N_2O film and the observed variation of the electronic absorption spectra as a function of deposition temperature, for 54 K $\leq T_d \leq$ 62 K. The analysis is extended to temperatures below 54 K to give new insight into the nature of phase change, from crystalline to amorphous, yielding an estimate of the physical extent of defect-free lattice as a function of T_d, on approaching a phase change at 47/48 K.

There is a long history of the influence of applied electric fields on the optical properties of solids, initiated by the discovery of the Franz–Keldysh effect.[9–19] The Franz–Keldysh effect is a change in absorption or reflectance of a solid with an applied or built-in field,[20] of typically a few $\times 10^6$ V m^{-1}. This may be accompanied by a shift to lower photon absorption energy.[13,17,21] Investigations of the effect have very largely, or indeed exclusively, been confined to semi-conductors. In the present work, a phenomenon is encountered which involves the influence of electric fields upon the optical spectra of solids, but one which is distinctively different from the Franz–Keldysh effect. First, we are concerned with an insulator, solid N_2O, with a bandgap of ~9.5 eV. Second, we observe a change in absorption energy with changing field, rather than a change in transmission or reflection. Moreover, the photon absorption energy increases with increasing electric field. Third, the properties of the exciton or

[a] *Department of Physics and Astronomy, Aarhus University, Ny Munkegade 120, DK-8000 Aarhus, Denmark. E-mail: amc@phys.au.dk*
[b] *School of Physical Sciences, The Open University, Walton Hall, Milton Keynes, MK7 6AA, UK*
[c] *Laboratoire Interuniversitaire des Systèmes Atmosphériques (LISA), CNRS UMR 7583, Universités Paris-Est Créteil and Paris Diderot, 61 avenue du Général de Gaulle, 94010 Créteil cedex, France*
[d] *ISA, Centre for Storage Ring Facilities, Department of Physics and Astronomy, Aarhus University, Ny Munkegade 120, DL-8000 Aarhus, Denmark*

hole–electron pair, created through the optical excitation of the solid, dominate the variation of the optical response of the material to the electric field.

2. Experimental details

Vacuum ultraviolet (VUV) absorption spectra for N_2O films were taken at the ASTRID2 Synchrotron Facility, Aarhus University, using the toroidal grating monochromator on the AU-UV beamline. This system provided tuneable polarised VUV, with a high-energy cut-off at 10.78 eV (115 nm), and was operated with a resolution of 0.075 nm throughout. The experimental chamber was fitted with a LiF entrance window, a MgF_2 substrate for film deposition, through which the beam was transmitted, and a MgF_2 exit window. The MgF_2 substrate was in thermal contact with a cold finger, cooled by a closed cycle helium cryostat and achieved a base temperature of 25 K. The temperature of the substrate could be set to any desired value and controlled to within $\pm$0.1 K using an Oxford Instruments controller.

The base pressure of the chamber was 10^{-9} mbar. N_2O was introduced *via* a 3 mm nozzle, 2 cm from the substrate. Films were grown at different substrate temperatures, T_d, by turning the heated substrate to face the gas nozzle. Film growth was monitored using an interference technique with a He–Ne laser,[2,22] enabling control of the film thickness to $\sim$9 nm or $\sim$30 monolayers (ML) for crystalline N_2O, given a refractive index = 1.421 to 1.425.[23] Experiments were carried out with the light beam at normal incidence to the film. Background spectra were collected through the clean MgF_2 substrate, giving the incident intensity $I_0(\lambda)$ in the range λ = 115 nm to 160 nm. Values of absorbance, that is, $\log_{10}(I_0(\lambda)/I(\lambda))$, as a function of incident wavelength, λ, were then recorded, where $I(\lambda)$ is the intensity of light transmitted through the film and substrate. Films display a maximum absorbance was $\leq\sim$0.35, ensuring that spectra were free from saturation, in a regime in which peak positions were independent of film thickness. All spectra were obtained and film growth performed with the sample at a constant temperature. Samples were annealed to 130 K to remove N_2O between experiments.

3. Results

Raw spectra for absorbance *vs.* λ are shown in Fig. 1, which displays spectra for independently prepared films of N_2O, each prepared at the T_d given. Spectra are offset on the absorbance scale for illustrative purposes, but show a maximum in the all data of $\sim$0.35, as mentioned above. The position of peaks in the spectra show clear dependence on T_d. Additional annealing experiments are also mentioned below, in Section 5.1.

In order to provide additional evidence for the hypothesis that these shifts in the VUV spectra of solid N_2O are due to the presence of the spontelectric field in the films, essentially identical experiments have been performed with solid films of CO_2. Since this species lacks a dipole moment, films are not expected to possess a spontelectric field.[7] Accordingly, no spectral

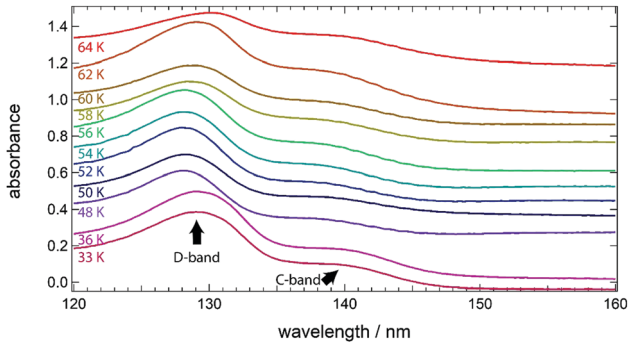

Fig. 1 Electronic absorption spectra of films of solid N_2O, for deposition temperatures, T_d, as marked, obtained on the ASTRID2 Synchrotron Facility, Aarhus University, using the AU-UV beamline at a resolution of 0.075 nm. Spectra, expressed as absorbance *vs.* wavelength, are displaced vertically for clarity. The maximum absorbance, lying in the D-band at 130 nm, is $\sim$0.35, see text.

shift should be observed with deposition temperature. This is illustrated in Fig. 2 for deposition temperatures of 40 K, 50 K and 60 K, covering temperatures of interest here. Fig. 2 shows that the positions of peaks in the absorption spectra are identical within measurement errors.

Spectral assignments, based upon gas phase spectra,[24] may be made for the two major peaks, marked C-band and D-band, in data for solid N_2O in Fig. 1. The gas phase dissociative structureless continuum at 130 nm, attributed to a Rydberg transition to the $D^1\Sigma^+$ state,[25] is represented in the solid state by a very similar band, henceforth the D-band. To longer wavelength, gas phase spectra show a partially resolved vibrational progression in the 140–160 nm region, assigned to the $C^1\Pi$ state. This state is blue-shifted by $\sim$6 nm in the solid state, with respect to the gas phase, and the vibrational progression is barely discernible for $T_d \geq$ 48 K. Vibrational structure is entirely washed out at T_d = 33 K or 36 K, emphasising the different structure of the solid at temperatures $<$48 K, corresponding to 'amorphous' N_2O.[26] This second lower energy peak will be

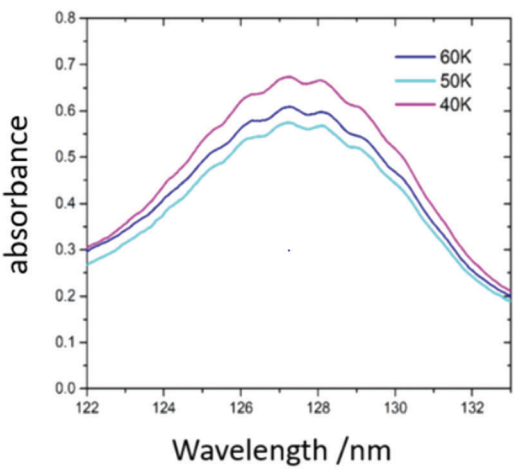

Fig. 2 Electronic absorption spectra of films of solid CO_2, for deposition temperatures, T_d, as marked. These are displaced for clarity, as in Fig. 1.

Table 1 C-Band data. Column 1: deposition temperature, T_d. Column 2: wavelength of maximum in the C-band, obtained through fitting to gaussians (see text). Column 3: observed shift from the peak at 54 K expressed in cm^{-1}. Column 4: calculated shift from the peak at 54 K (eqn (3)). Values for $T_d < 54$ K are discussed in Section 3. Column 5: the shift in the hole–electron separation due to the presence of the spontelectric field, Δr. Values for $T_d < 54$ K assume the absence of traps in the material (see text). Column 6: the hole–electron separation in the presence of the spontelectric field, $r + \Delta r$, assuming the absence of traps in the material. Column 7: the spontelectric field corresponding to the deposition temperature.[7] Values are corrected for layer spacing, s, reported in[26]

T_d/K	Wavelength/nm	Shift from 54 K/cm^{-1} ± 5 cm^{-1}	Calculated shift from 54 K/cm^{-1}	Δr/nm	$r + \Delta r$/nm	Spontelectric field, E_S/V m^{-1}
48	137.95	5	—	3.929	5.811	7.324×10^7
50	138.93	517	—	2.071	3.953	6.319×10^7
52	138.10	83	—	1.508	3.390	5.652×10^7
54	137.94	0	—	1.242	3.124	5.206×10^7
56	138.33	205	216	1.079	2.961	4.871×10^7
58	138.71	401	388	0.941	2.823	4.540×10^7
60	138.96	532	548	0.785	2.667	4.104×10^7
62	139.34	727	695	0.595	2.477	3.454×10^7
64	140.62	1379	890	0.374	2.256	2.483×10^7

referred to below as the C-band. The associated $^1\Pi$ excited state again has some Rydberg character.[25]

Spectra in Fig. 1 have been fitted with three overlapping gaussians, one to reproduce the C-band profile at ~139 nm, a second for the D-band at ~129 nm and a third to take account of the background contribution arising from the wavelength cut-off at 115 nm. The C-band and D-band gaussians were constrained to a full-width half maximum (FWHM) of <10 nm, whereas the background contribution was unconstrained, but typically assumed a FWHM of 16 nm, centred around 121 nm. The resulting peak positions are recorded in Tables 1 and 2. Errors in peak positions of ± 0.01 nm translate into errors in shifts of ± 5 cm^{-1}.

The spectra in Fig. 1 show that the vibrational states for solid N_2O are not resolved. We assume of necessity that the excitons in the D- and C-states may be treated independently of the vibrational state of the excited state. This is equivalent to the standard separation of the wave function into independent electronic and vibrational parts. Further, any potential Davydov splitting is unresolved, noting that it is likely to be small for a FCC system such as N_2O.[27]

Table 2 D-Band data. Column 1: deposition temperature, T_d. Column 2: wavelength of maximum in the D-band, obtained through fitting to gaussians (see text). Column 3: observed shift from the peak at 52 K expressed in cm^{-1}. Column 4: calculated shift from the peak at 52 K (eqn (3)). Column 5: the shift in the hole–electron separation in the presence of the spontelectric field, Δr. Values for $T_d < 52$ K assume the absence of traps in the material (see text). Column 6: the hole–electron separation in the presence of the spontelectric field, assuming the absence of traps in the material

T_d/K	Wavelength/nm	Shift from 52 K/cm^{-1}	Calculated shift from 52 K/cm^{-1}	Δr/nm	$r + \Delta r$/nm
48	128.50	0	—	1.452	3.131
50	128.50	0	—	1.029	2.708
52	128.50	0	—	0.825	2.504
54	128.60	61	154	0.712	2.391
56	128.80	181	251	0.637	2.316
58	129.00	302	335	0.569	2.248
60	129.20	422	428	0.488	2.167
62	129.50	601	538	0.382	2.061
64	130.30	1075	651	0.249	1.928

4. Analysis

Our purpose here is to model the variation in peak positions in absorption spectra of solid N_2O with deposition temperature, T_d, shown in Fig. 1 and Tables 1 and 2. First we note that, from $T_d \geq 52$ K (D-band) or 54 K (C-band), there is a shift in wavelength of peak absorption to the red as T_d increases to 64 K, that is, as the spontelectric field decreases. Throughout, shifts are recorded relative to 54 K for C-band or 52 K for D-band. Thus the smaller the value in column 3 of Tables 1 and 2, the greater the displacement of the peak position from some putative zero field value. By contrast with higher temperature data, the peak absorption wavelength for films deposited at 50 K and 52 K shifts to the blue relative to 54 K in the C-band, whereas in the D-band the wavelength remains unchanged at these deposition temperatures. Spectra for $T_d < 48$ K are illustrated by data for $T_d = 33$ K and 36 K in Fig. 1 and show that spectra are unchanged with temperature in this lower temperature range, but are shifted to the red, compared with higher temperatures.

When crystalline solids absorb radiation in the visible and UV or VUV, excitons are formed which may be divided into the categories of Frenkel, Wannier–Mott and charge-transfer. In the strongly bound Frenkel excitons, the electron and hole are local to the excited atom or molecule, whereas in weakly bound Wannier–Mott excitons, the electron–hole separation is large in comparison with the separation between the constituent atoms or molecules of the crystal. Charge-transfer excitons and other examples constitute intermediate cases.[18,28,29] In molecular crystals, such as here, the Frenkel model, based upon HOMO–LUMO electronic excitation in the isolated molecule, is generally adopted. Wannier–Mott excitons have been considered as confined to semiconductors, and excluded in high band gap, low electrical permittivity species, with some rare exceptions of intermediate band gap for example for LiH.[30] However recent work on solid CO, with a band gap of >8 eV and a permittivity of ~1.42, showed that Wannier–Mott excitons can be excited in this material.[1] This conclusion was based on the known variation of spontelectric field with temperature in solid CO.[31] This variation was used to reproduce the dependence of VUV photon absorption energy with film deposition temperature, using a simple electrostatic model of the action of the spontelectric field on a Wannier–Mott exciton, reviewed below and employed here.[1]

Various mechanisms, other than the action of the spontelectric field, may also in principle contribute to the shifts recorded in Tables 1 and 2. As discussed in ref. 1, these involve (i) the permanent dipole moment change in N_2O associated with the Stark shift between the X and C or D state, (ii) the

induced dipole moment change through polarizability changes between the X and C or D state, (iii) changes in the average degree of dipole orientation associated with changes in the deposition temperature, T_d. Although estimates of the relevant quantities, such as the polarizabilities and dipole moments of N_2O in C and D states, are unavailable, it is evident from the discussion in ref. 1 that these mechanisms contribute negligibly to the observed spectral shifts in Tables 1 and 2. For example, with regard to point (iii), above, we note that the energy of interaction between two dipoles, each of value μ, at an angle θ to one another and at a distance r_{12} apart, may be expressed in SI as $-[\mu^2/(4\pi\varepsilon_0 r_{12}{}^3)](1 - 3\cos^2\theta)$. A layer spacing of $s = 0.2905$ nm, defined as the distance between dipoles in the z-direction,[25] leads to $\mu_{N_2O} = 0.0671$ D in the solid state, where depolarization reduces the gas phase value through a factor $(1 + \alpha k/s^3)$, using $k = 11.034$ and a polarizability $\alpha = 3.31 \times 10^{-30}$ m^3.[7] Average values of θ at 52 K and 60 K are respectively 85.2° and 86.7° to the normal to the surface, given by the inverse cosine of experimental values of the degree of dipole orientation for these temperatures.[7] This suggests a shift in interaction energies between adjacent N_2O species of <0.01 cm^{-1} between 52 K and 60 K.

Returning to the influence of the spontelectric field on the N_2O excitonic state, we first note that fully quantum mechanical analysis of excitons, in applied fields of several MV m^{-1}, has been performed, for example for GaN.[16] We find here however that a straightforward classical model is sufficient to reproduce the spectra shifts in Tables 1 and 2 with some fidelity, as we found for solid CO.[1] As the temperature of film deposition is lowered, the Wannier–Mott exciton, formed in VUV excitation, is subjected to a higher electric field. This drives the electron–hole pair successively further apart. This may be expressed analytically in a straightforward classical manner under the assumptions, consistent with the presence of Wannier–Mott excitons, that (i) the electron–hole separation is very much greater than the intermolecular separation in the crystal, and following this, (ii) the electrical permittivity may be assumed to be that of the bulk material and (iii) the only significant mutual interaction between the hole and electron is the Coulomb attraction.[1]

Let the electron–hole separation in the hypothetical absence of the spontelectric field be r, where the value of r is characteristic of the transition involved. Thus, using atomic units throughout (*e.g.* $\varepsilon_0 = 1/4\pi$, electronic charge = 1), the force between the hole and electron = $1/r^2$. In the presence of the spontelectric field, E_S, given in Table 1, r increases to $r + \Delta r$ and the force becomes $1/(r + \Delta r)^2$. The force on the hole and electron is E_S on each and thus the additional force experienced by the hole and electron = $2E_S$. This is balanced by the change in coulombic force. Hence

$$1/(\varepsilon r^2) - 1/[\varepsilon\,(r + \Delta r)^2] = 2E_S \qquad (1)$$

where ε is the permittivity of the bulk material. This may now be solved for Δr to yield

$$\Delta r_i = r[(1 - 2E_i\varepsilon r^2)^{-1/2} - 1] \qquad (2)$$

Eqn (1) and (2) were also introduced in ref. 1. Moving a charge a distance Δr, in a field E, changes the energy by $\Delta r{\cdot}E$. Therefore at temperature T_i, the change in energy is $\Delta r_i{\cdot}E_i$ and at temperature T_j, the change is Δr_jE_j. Since both charge and hole move equally and in opposite directions, the total change in energy = $2\Delta r_i{\cdot}E_i$ or $2\Delta r_jE_j$. Therefore the energy shift between temperatures T_i and T_j, = $2(\Delta r_i{\cdot}E_i - \Delta r_jE_j)$, is given by

$$\Delta\mathscr{E}_{ij} = 2r\{(1 - 2E_i\varepsilon r^2)^{-1/2}\,E_i - (1 - 2E_j\varepsilon r^2)^{-1/2}E_j - (E_i - E_j)\} \qquad (3)$$

The term $E_i - E_j$ was excluded in the expression given in ref. 1, through the use of an average field, *post hoc* an unnecessary approximation. We note in passing that inclusion of this term for solid CO, as in ref. 1, changes the calculated shifts by $\sim$1%.

The value of the bulk permittivity, ε, in eqn (3), is not a directly measured quantity for solid N_2O, but may be estimated as follows. The relationship between the gas phase and the solid-state dipole moment, μ_0 and μ, simulates the response of the medium to an applied field.[7] Thus we set $\varepsilon = (1 + \alpha k/s^3) = 2.489$ on inserting values for the polarizability, α, the layer spacing, s and k given above, thus ensuring that the current analysis is consistent with the spontelectric fields shown in Table 1. In addition, the value of ε is negligibly affected by the spontelectric field in the medium.[32] This is in accord with the Johnson relation,[33] valid for a polarization of <0.01 C m^{-2}, where the current value is of the order of 10^{-3} C m^{-2}. Numerical experiments in fact show that the shifts in absorption energy, calculated using eqn (3), are insensitive to the value of ε chosen and suffer no significant change if the generic low temperature value of $\varepsilon = 2$ is used to replace 2.489. We note that the value of ε may also be estimated from the square of the refractive index to lie between 2.02 and 2.03.[22]

In order to determine r, the separation of the hole and electron in the absence of the spontelectric effect, pairs of deposition temperatures, T_d, were taken. Eqn (3) then yields a value of r of 35.6 $\pm$ 0.27 au or 1.88 $\pm$ 0.01 nm, for the C-state and 31.7 $\pm$ 4.3, or 1.68 $\pm$ 0.23 nm, for the D-state, where values of $r = 1.88$ nm and 1.68 nm have been chosen on a least squares basis to fit the observations. Uncertainties quoted represent the spread of values of r obtained in taking the various pairs of deposition temperatures. Evidently the value of r should be independent of T_d for any electronic state. Thus the greater spread associated with the D- compared with the C-state indicates a poorer fit of the model to the data, as we find below. Inserting these values of r, eqn (2) also yields the values of physical displacement, Δr_i, *versus* T_d. These are shown in Tables 1 and 2 for the C- and D-states respectively. These give an observed size, $r + \Delta r_i$, of the hole–electron pair of 3.124 nm at 54 K for the C-state and 2.504 nm at 52 K for the D-state, representing respectively 10.75 and 8.62 layer spacings, s. These figures are typical of conventional Wannier–Mott excitons. We note that the measured spectral shifts below 54 K for the C-state and below 52 K for the D-state imply that some other phenomenon is governing the physics in the low temperature regime; this is the focus of the discussion below. The size of the hole–electron pairs is, however, maximised at these temperatures for the respective states. Values of displacement, Δr_i, show

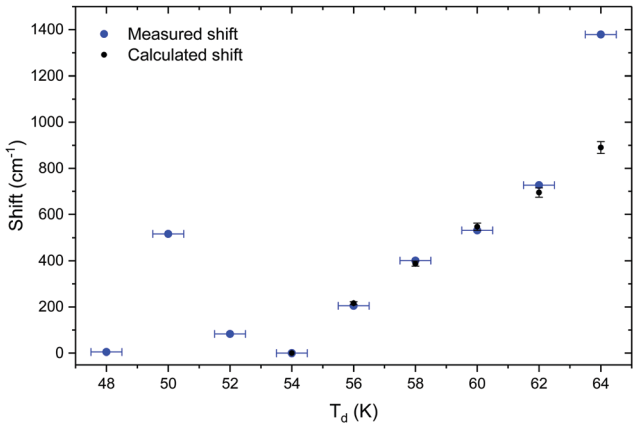

Fig. 3 Values of calculated and measured shifts, in cm^{-1}, for the C-band of solid N_2O *vs.* temperature of deposition, T_d, where calculated values are obtained using eqn (3). Shifts are relative to the value at T_d = 54 K. Errors in the calculated shifts stem from uncertainties in the value of the size of the excitons, *r*, in the absence of a spontelectric field. An experimental uncertainty of ±0.5 K is ascribed to T_d.

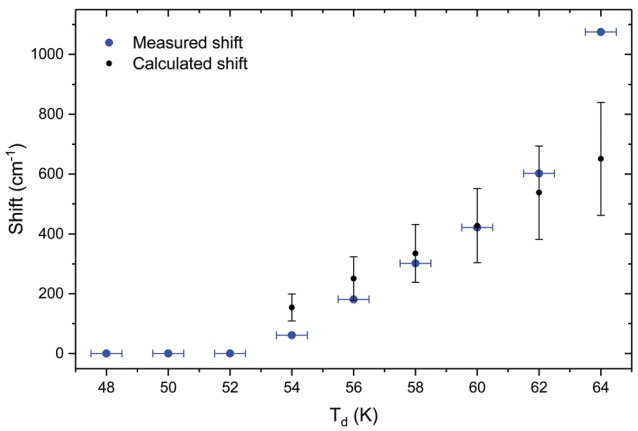

Fig. 4 Values of calculated and measured shifts, in cm^{-1}, for the D-band of solid N_2O *vs.* temperature of deposition, T_d, where calculated values are obtained using eqn (3). Shifts are relative to the value at T_d = 52 K. Uncertainties in the value of '*r*', obtained from a comparison of values obtained from each pair of temperatures, is greater than for C-band data and translates into ±29% in the calculated shifts.

the expected fall with increasing T_d, that is, with decreasing spontelectric field.

Fig. 3 and 4 show the results for calculated redshifts for bands C- and D-, obtained using eqn (3), compared with the experimental values. Values are also given in Tables 1 and 2. In order to estimate the uncertainty in the calculations, we have included the effect of ±1% uncertainty in the value of *r* for the C-state and ±10% uncertainty for the D-state, using the ranges given above. These uncertainties give rise in turn to an error of ∼3% in the shifts calculated for the C-band and ∼30% in those for the D-band.

5. Discussion

Results in Section 4 broadly support the model of Wannier–Mott exciton sensitivity to the spontelectric field. Agreement between model and observation, in Fig. 3 and 4, is however restricted to T_d = 54–56 K to 62 K. The most obvious discrepancy is that whilst the spontelectric field increases below T_d = 54 K or 56 K to 48 K, column 7 of Table 1, the spectral shift does not follow suit. The data at 64 K also cannot be reconciled with the model described in Section 3.

5.1 Exciton concentrations, exciton diffusion and exciton blockade

We propose that the expansion of the exciton diameter, Δr, in Tables 1 and 2, suffers a blockade when the value of the diameter reaches the value of 3.124 nm in the C-state, at 54 K, and 2.504 nm, at 52 K, in the D-state. We first consider the number density of excitons created in our experiments and demonstrate that their mutual interaction cannot lead to the observed behaviour of spectra at $T_d < 54$ or 52 K. We then discuss how the formation of defects offers a possible explanation for our observations.

An area of the film, *A*, = 2.5 × 10^{-5} m^2, is irradiated with I_0 = 1.2 × 10^{10} incident photons per second in the 0.075 nm bandwidth of the light. Using a maximum absorbance $\alpha \sim 0.35$ at 130 nm, the steady state exciton concentration, [X], is given by $I_0 t_e(1 - e^{-\alpha})/V$, where *V*, the volume of the film, is given by its area, *A* × thickness and t_e is the lifetime to decay of the exciton. Using a film thickness of 9 nm, and assuming a generic value of t_e of 1 ns,[34] yields [X] ∼1.6 × 10^7 cm^{-3}. This estimate implies that there is 1 exciton in 6.25 × 10^{-14} m^3 on average, equivalent crudely to a separation of $(6.25 \times 10^{-14})^{1/3} \sim 4 \times 10^{-5}$ m. The maximum size of the exciton, found in the C-band for films deposited at 54 K, is ∼3 × 10^{-9} m (Table 1). On this basis, there is no contact annihilation and accompanying ionization. In addition, although such excitons have a large dipole moment of 9.1556 × 10^{-28} C m, their maximum mutual dipole–dipole interaction is negligible and equal to ∼6 × 10^{-9} cm^{-1} at a separation of r_{12} = 4 × 10^{-5} m, using an interaction energy = $|[\mu^2/(2\pi\varepsilon_0\varepsilon r_{12}{}^3)]|$.

Excitons however diffuse in the solid and we now ask whether such diffusion could lead to interactions between them. With an assumed temperature independent diffusion coefficient, *D*, of a few × 10^{-4} m^2 s^{-1},[35,36] this gives a diffusion distance of $(2Dt_e)^{1/2} \sim 1.4$ μm, using for example *D* = 7 × 10^{-4} m^2 s^{-1}, the value for ZnO[34] and t_e of 1 ns, as above. Alternatively, an effective velocity of travel of 10^3 ms^{-1}, suggested in[33] for Wannier–Mott excitons within solids, yields a similar value of ∼1 μm. This may be compared with the above estimate of the separation of ∼40 μm, based on the concentration of excitons in our sample. Notwithstanding the uncertainties in our estimates, we conclude that exciton–exciton collisions are essentially absent and are not the origin of the blockade in the absorption wavelength shift with decreasing T_d.

In order to understand how the proposed blockade may arise, we turn to structural changes in the film with deposition temperature. It is known, through reflection–absorption infrared spectroscopy (RAIRS)[37] and neutron scattering data, that solid N_2O exists as a crystalline film when deposited above 48 K, but as a more amorphous film when deposited with $T_d < 47$ K.

Neutron scattering data[26] also showed that annealing a N_2O film, of thickness 10 nm, from 20 K to 47 K, in the 'amorphous' phase, causes the density of the film to drop from 1.57 ± 0.03 g cm^{-3} to 1.47 ± 0.03 g cm^{-3} and the film thickness increases from 10 nm to 11.5 nm. At 50 K, the density partially recovers to 1.51 ± 0.03 g cm^{-3} and at 53 K the film thickness moves back to 10 nm.

We suggest that these structural differences between films, prepared as T_d decreases from 54 K, result in the formation of defects, which act as traps to excitons. It is well known that a structural defect can capture free electrons[18,38] and here we extend this concept to the immobilization of weakly bound electrons associated with Wannier–Mott excitons.[39] Thus, for the C-state (Table 1), traps form at T_d = 54 K with a characteristic separation of 3.124 nm and that further expansion of the exciton to greater size under the influence of the spontelectric field is therefore inhibited. A further breakdown of structure takes place at 52 K, leading to a blockade in the D-state exciton expansion, with a characteristic trap separation of 2.504 nm.

For the C-state, a reversal of the shift may be seen in Table 1 for T_d = 52 K and 50 K, where shifts take on values of $\Delta E_{ij} = -83$ and -517 cm^{-1} respectively, relative to 54 K. Here the blockade is sufficiently powerful that the shift reverses in value compared with T_d = 54 K, indicating that the restriction in size of the exciton imposed by the blockade overcomes the effect of the greater electric field at lower temperatures. Using r = 1.88 ± 0.01 nm, as derived above for the C-state, we may estimate Δr_{50} and Δr_{52} as follows. The measured shift ΔE_{ij} is given by:

$$\Delta E_{ij} = 2[(r + \Delta r_{50})_C E_{50} - (r + \Delta r_{54})_C E_{54}] = -517 \text{ cm}^{-1} \quad (4)$$

and

$$\Delta E_{ij} = 2[(r + \Delta r_{52})_C E_{50} - (r + \Delta r_{54})_C E_{54}] = -83 \text{ cm}^{-1} \quad (5)$$

where the C-subscript signifies that quantities refer to the C-state. This yields Δr_{50} = 0.185 nm and Δr_{52} = 0.904 nm for the C-state. Therefore $(r + \Delta r_{50})_C$, the effective diameter of the C-state exciton for T_d = 50 K, is 2.07 ± 0.01 nm and for 52 K, $(r + \Delta r_{52})_C$ is 2.78 ± 0.01 nm. Thus the exciton diameter shrinks progressively between 54 K, 52 K and 50 K from 3.12, 2.78 to 2.07 nm respectively, on the basis of the C-band data. The D-band data restrict the diameter to 2.504 nm at 52 K (Table 2). The D-state exciton shows zero shift between T_d = 52 K and 50 K (Table 2), giving Δr_{50} = 0.561 nm. Using r_D = 1.68 ± 0.23 nm, we obtain $(r + \Delta r_{50})_D$ = 2.24 ± 0.23 nm. The equality, within experimental error, between $(r + \Delta r_{50})_C$, = 2.07 nm, and $(r + \Delta r_{50})_D$ is to be expected, since both the C- and D-state excitons are restricted by the same structural blockade. We conclude therefore that the diameter of the exciton shrinks from 3.124 nm at 54 K, to 2.504 nm at 52 K and to 2.07 nm at 50 K, values shown in Table 3.

The above suggests a successively higher defect or trap concentration as the film growth temperature approaches the critical temperature of 47/48 K, below which an amorphous phase of nitrous oxide begins to dominate in the film. For example, the concentration of traps increases by a factor of $(3.124/2.504)^3 \sim 1.9$ in the temperature range T_d = 54 K to 52 K and a factor of $(3.124/2.07)^3 \sim 3.4$ between 54 K and 50 K. Defect and trap formation may represent a precursor to phase change. Our results may be seen to follow the general concept of Ostwald's 'rule of stages' in which any system undergoes a phase change through a series of intermediate metastable states into the most thermodynamically stable state, rather than in a single direct step.[40–42] We note that diffusion of excitons will also be inhibited by the presence of traps.

Table 3 Column 1: temperature of deposition. Column 2: the diameter of the corresponding exciton. Column 3: the number of unit cells of defect free FCC N_2O contained within the volume of the exciton. Column 4: the corresponding number of molecules contained within the defect free structure. Column 5: the origin of data used to obtain values shown

T_d/K	$d = r + \Delta r$/nm	Number of unit cells	Number of molecules	Data
50	2.07 ± 0.01	23.7 ± 0.2	95 ± 1	C-Band
52	2.50 ± 0.23	42 ± 11.5	168 ± 46	D-Band
54	3.12 ± 0.01	81 ± 0.75	324 ± 3	C-Band

Turning to data at T_d = 64 K, this temperature is close to the highest value, of 65 K, at which N_2O may be condensed to form a film.[7] The current model breaks down and the shift, ΔE_{ij}, shows discrepancies of -489 cm^{-1} from that predicted by eqn (3), for the C-state and -424 cm^{-1} for the D-state (Tables 1 and 2). Moreover the spontelectric fields in films formed at T_d = 64 K are a factor of ~2 lower in value than the predictions of the spontelectric model, otherwise generally accurate at lower temperatures.[25] Expansion of the exciton is doubtless inhibited by loss of structural integrity at this limiting temperature, but it is not possible to make more than this qualitative statement.

Further evidence for the existence of traps, and exciton blockade, within solid films of N_2O is provided through experiments in which films were deposited at 33 K and annealed in a series of 1 K to 2 K steps, with spectra recorded at each temperature. In this connection, note that annealing is both qualitatively and quantitatively different from deposition at a series of temperatures, T_d. For example, the spontelectric field within the film remains largely unchanged on annealing.[7] With this in mind, we find that the position of absorption bands remains constant on annealing between 33 K and 44 K but, as the temperature of phase change approaches, the wavelength moves abruptly, between 44 K and 48 K, from 139.8 nm to 138.7 nm for the C-state and 129.7 nm to 128.6 nm for the D-state, equivalent to a blue-shift of ~600 cm^{-1} in each case. This may be interpreted as indicative of progressive annealing of traps above 44 K, allowing the presence of the spontelectric field to make itself felt and the excitons accordingly to expand, through dissipation of the blockade.

5.2 Dimensions of defect-free regions

The analysis in Section 5.1 allows estimation of the size of the defect-free regions, with associated long-range periodicity, which give rise to exciton formation and the variation of this size with deposition temperature.[43] This is an issue which has been addressed in individual crystallites[44] with regard to band structure, but little discussed for defect-free regions embedded in a bulk crystal.[45]

The layer spacing, s, in an FCC lattice is half the dimension of the unit cell and thus the unit cell volume = $8s^3$. Writing the exciton diameter $d = r + \Delta r$, the exciton volume, assumed spherical for the present purposes, is given by $\pi d^3/6$. The number of unit cells contained within this volume is therefore given by $\pi/48\ (d/s)^3$. Using d = 3.124 nm and 2.504 nm, for the C-state (T_d = 54 K) and D-state (T_d = 52 K) excitons respectively, and s = 0.2905 nm,[25] the number of unit cells encompassed by the C-state exciton is 81 ± 0.75, for T_d = 54 K, and for the D-state is 42 ± 11.5, for T_d = 52 K. At 50 K, the number of unit cells falls to 23.7± 0.2, using d = 2.07 ± 0.01 nm, derived from C-state data above.

Given that there are 4 molecules per unit cell in a FCC lattice,[46] this analysis gives a series of estimates for the number of molecules involved in a regular defect-free conformation *vs.* deposition temperature, in N_2O films. Thus at 54 K, the number of molecules is 324 ± 3 molecules. At 52 K, the figure is 168 ± 46 molecules and at 50 K, the figure is 95 ± 1 molecules. These results are collated in Table 3. Note that these structures are defect free regions within a solid on the nanometre-scale, as opposed to individual nanocrystals or molecular clusters, for which quantum confinement effects lead to a continuous blue-shift in the spectrum with decreasing crystallite size.[43,47]

6. Concluding comments

The data reported here show that the blueshift in electronic absorption spectra of solid N_2O, with decreasing deposition temperature, is due to the spontelectric effect in films of this material. Results therefore corroborate the finding of a similar effect reported for CO.[1] The analysis, for both CO and N_2O, is based on the presence of Wannier–Mott excitons in a high band gap insulator, with a low relative permittivity. Data therefore provide further evidence that weakly bound excitons of this nature can form in these materials.

Our interpretation of the VUV absorption spectra of solid N_2O is that the material forms metastable states, identified at 54 K, 52 K and 50 K, in its path to the phase change at 47/48 K.[26] These metastable states are estimated to contain defect-free islands of 324 ± 3, 168 ± 46 and 95 ± 1 N_2O molecules, at these three deposition temperatures. This evokes an image of the formation of defect-free regions of ever decreasing extent, Table 3, as the temperature approaches that of the phase change. Each defect-free region is limited in dimension by surrounding structural defects, which act as a shrinking cage, as the temperature drops. At 48 K, extrapolation yields a region corresponding to a few unit cells, behaviour which may be regarded as signalling the phase change. One may note that the formation of defects appears to have no discernible effect on the spontelectric field generated within the film, just as the major disruption of structure at 48 K creates no discontinuity in the electrical polarization.[26] The results mentioned encapsulate the additional significance of the current work compared with the related work on CO.[1] Here we are able to formulate a graphic and quantitative mechanism for the processes that occur as we approach a phase change. This is a novel aspect that was lacking in the work involving solid CO.

The current study suggests two areas of future research. The first is to investigate if a relationship can be found between the size of defect-free structures and parameters associated with film growth, such as rate of background dosing, beam dosing or substrate material. The second would be to attempt to identify the Franz–Keldysh effect in spontelectric materials.

Conflicts of interest

There are no conflicts to declare.

Acknowledgements

We should like to acknowledge the Centre for Storage Ring Facilities at Aarhus (ISA) for granting access to the AU-UV beamline on the ASTRID2 storage ring and the staff at ASTRID2 for their technical assistance in performing our experiments, with special thanks to Nykola Jones. The research leading to this result has been supported by the project CALIPSOplus under the Grant Agreement 730872 from the EU Framework Programme for Research and Innovation HORIZON 2020.

References

1 Y.-J. Chen, G. Muñoz Caro, S. Aparicio, A. Jiménez-Escobar, J. Lasne, A. Rosu-Finsen, M. R. S. McCoustra, A. M. Cassidy and D. Field, *Phys. Rev. Lett.*, 2017, **119**, 157703.
2 A. Dawes, R. J. Mukerji, M. P. Davies, P. D. Holtom and S. M. Webb, *et al.*, *J. Chem. Phys.*, 2007, **126**, 244711.
3 G. M. Muñoz Caro, Y.-J. Chen, S. Aparicio, A. Jiménez-Escobar, A. Rosu-Finsen, J. Lasne and M. R. S. McCoustra, *Astron. Astrophys.*, 2016, **A19**, 589.
4 R. Balog, P. Cicman, N. C. Jones and D. Field, *Phys. Rev. Lett.*, 2009, **102**, 2–5.
5 O. Plekan, A. M. Cassidy, R. Balog, N. C. Jones, J. Dunger and D. Field, *Phys. Chem. Chem. Phys.*, 2011, **13**, 21035–21044.
6 D. Field, O. Plekan, A. M. Cassidy, R. Balog and N. C. Jones, *Europhys. News*, 2011, **42**, 32–35.
7 D. Field, O. Plekan, A. N. Cassidy, R. Balog, N. C. Jones and J. Dunger, *Int. Rev. Phys. Chem.*, 2013, **32**, 345–392.
8 O. Plekan, A. Rosu-Finsen, A. M. Cassidy, J. Lasne, M. R. S. McCoustra and D. Field, *Eur. Phys. J. D*, 2017, **71**, 162–180.
9 L. V. Keldysh, *Sov. Lett. JETP*, 1965, **20**, 1307.
10 W. Franz, *Z. Naturforsch., A: Phys. Sci.*, 1958, **13A**, 484.
11 K. W. Böer, H. J. Hänsch and U. Kümmel, *Naturwissenschaften*, 1958, **19**, 460.
12 B. O. Serpahin and R. B. Hess, *Phys. Rev. Lett.*, 1965, **14**, 654.
13 K. Wakita, Electroabsorption Effect, *Semiconductor Optical Modulators*, Springer, Boston, MA, 1998.
14 M. Schmid, M. Oehme, M. Kaschel, J. Werner, E. Kasper and J. Schulze, *Franz–Keldysh effect in germanium pin*

photodetectors on silicon, 7th IEEE International Conference on Group IV Photonics, Beijing, 2010, pp. 329–331.
15 D. E. Aspnes, *Phys. Rev.*, 1966, **147**, 554.
16 F. L. Lederman and J. D. Dow, *Phys. Rev. B: Condens. Matter Mater. Phys.*, 1976, **13**, 1633.
17 S. Lenk and E. Runge, *J. Phys.: Conf. Ser.*, 2010, **210**, 012047.
18 H. Garcia, *Phys. Rev.*, 2006, **74**, 05212 and references therein.
19 C. Kittel, *Introduction to Solid State Physics*, John Wiley&Sons, New York, London, Sydney, 7th edn, 2007.
20 Y. Turkulets and I. Shalish, 2018, *arXiv:1803.10275v2[physics. app-ph]*.
21 F. Novelli, D. Fausti, F. Giusti, F. Parmigiani and M. Hoffmann, *Nat. Sci. Rep.*, 2013, **3**, 1227.
22 A. Dawes, M. Pascual, S. V. Hoffmann, N. C. Jones and N. J. Mason, *Phys. Chem. Chem. Phys.*, 2017, **19**, 27544.
23 R. L. Hudson, M. J. Loeffler and P. A. Gerakines, *J. Chem. Phys.*, 2017, **146**, 024304.
24 J. B. Nee, J. C. Chang, P. C. Lee, X. Y. Wang and C. T. Kuo, *Chin. J. Phys.*, 1999, **37**, 172.
25 D. G. Hopper, *J. Chem. Phys.*, 1984, **80**, 4290.
26 A. M. Cassidy, M. R. V. Jørgensen, A. Rosu-Finsen, J. Lasne, J. H. Jørgensen, A. Glavic, V. Lauter, B. B. Iversen, M. R. S. McCoustra and D. Field, *J. Phys. Chem. C.*, 2016, **120**, 24130.
27 D. Fox and R. M. Hexter, *J. Chem. Phys.*, 1964, **41**, 1125.
28 E. Baldini, L. Chiodo, A. Dominguez, M. Palumno and S. Moser, *et al.*, *Nat. Commun.*, 2017, **8**, 13.
29 P. Cudazzo, F. Sottile, A. Rubio and M. Gatti, *J. Phys.: Condens. Matter*, 2015, **27**, 113204.
30 V. G. Plekhanov, *Rep. Prog. Phys.*, 1998, **61**, 1045.
31 J. Lasne, A. Rosu-Finsen, A. M. Cassidy, M. R. S. McCoustra and D. Field, *Phys. Chem. Chem. Phys.*, 2015, **17**, 30177.
32 C. Ang and Z. Yu, *Phys. Rev.*, 2004, **69**, 174109.
33 K. M. Johnson, *J. Appl. Phys.*, 1962, **33**, 2826.
34 D. C. Reynolds and T. C. Collins, *Excitons, their properties and uses*, Academic Press, 1981.
35 M. Shahmohammadi, G. Jacopin, X. Fu, D.-D. Ganière, D. Yu and B. Deveaud, *Appl. Phys. Lett.*, 2015, **107**, 141101.
36 L. Yuan, T. Wang, T. Zhu, M. Zhou and L. Huang, *J. Phys. Chem. Lett.*, 2017, **8**, 3371.
37 J. Lasne, A. Rosu-Finsen, A. Cassidy, M. R. S. McCoustra and D. Field, *Phys. Chem. Chem. Phys.*, 2015, **17**, 20971.
38 M. Ueta, H. Kanzaki, K. Kobayashi, Y. Toyozawa and E. Hanamura. *Excitonic Processes in Solids*, Solid Sate Sciences 60, Springer Series, 2012.
39 S. V. Izvekov and V. I. Sugakov, *Phys. Status Solidi B*, 1995, **191**, 449.
40 S.-Y. Chung, Y.-M. Kim, J.-G. Kim and Y.-J. Kim, *Nat. Phys.*, 2009, **5**, 68.
41 A. Levin, T. O. Mason, L. Adler-Abramovich, A. K. Buell and G. Meisl, *et al.*, *Nat. Commun.*, 2014, **5**, 5219.
42 Y. Li, L. Zhang, D. L. Jacobs, J. Zao, X. Yue and C. Wang, *Nat. Commun.*, 2017, **8**, 14462.
43 K. W. Böer and U. W. Pohl, *Bands and Bandgaps in Solids. In: Semiconductor Physics*, ISBN 978-3-319-69149-7 Springer, 2018.
44 L. Brus, *J. Phys. Chem.*, 1986, **90**, 2555.
45 S. B. Hasan, E. Yeganegi, A. P. Mosk, A. Legendijk and W. Vos, *Phys. Rev. Lett.*, 2018, **120**, 237402.
46 W. C. Hamilton and M. Petrie, *J. Phys. Chem.*, 1961, **65**, 1453.
47 R. E. Marotti, P. Giorgio, G. Macado and E. A. Dalchiele, *Sol. Energy Mater. Sol. Cells*, 2006, **90**, 2356.